

Improved performance of an ultrastable measurement platform using a field-programmable gate array for real-time, deterministic control

Allison B. Churnside^{ab}, Gavin M. King^a, Ashley R. Carter^{ab}, Thomas T. Perkins^{*ac}

^aJILA, National Institute of Standards and Technology and University of Colorado, Boulder, CO, USA 80309

^bDept. of Physics, ^cDept. of Molecular, Cellular, and Developmental Biology, University of Colorado, Boulder, CO, USA 80309

ABSTRACT

Many precision measurement techniques (e.g. scanning probe microscopy, optical tweezers) are limited by sample drift. This is particularly true at room temperature in air or in liquid. Previously, we developed a general solution for sample control in three dimensions (3D) by first measuring the position of the sample and then using this position in a feedback loop to move a piezo-electric stage accordingly (Carter *et al.*, Optics Express, 2007). In that work, feedback was performed using a software-based data acquisition program with limited bandwidth (≤ 100 Hz). By implementing feedback through a field programmable gate array (FPGA), we achieved real-time, deterministic control and increased the feedback rate to 500 Hz – half the resonance frequency of the piezo-electric stage in the feedback loop. This better control led to a three-fold improvement in lateral stability to 10 pm ($\Delta f = 0.01$ -10 Hz). Furthermore, we exploited the rapid signal processing of FPGA to achieve fast stepping rates coupled with highly accurate and orthogonal scanning.

Keywords: Optical traps, optical tweezers, atomic force microscopy, scanning probe microscopy

1. INTRODUCTION

Atomic-scale sensing lies at the heart of a variety of high-resolution microscopies.¹⁻⁴ Yet, such high sensitivity without similar positional stability limits the utility of these techniques.⁵⁻⁷ Environmental perturbations (e.g. temperature, acoustic, liquid) lead to unmeasured drift. As shown in Figure 1a, the position of a microscope stage drifted at a ~ 2 nm/min before the stabilization was turned on ($t < 0$). Extreme stability can be achieved passively in highly controlled environments. For example, the pinnacle of picoscale control for scanning probe microscopy (SPM) is achieved using instruments that are secluded from the perturbative environment by multiple layers of isolation and that operate at low temperature and ultrahigh vacuum. These impressive levels of isolation achieve drift rates of ~ 1 pm/min.⁸ However, many applications, for instance biological studies, demand room-temperature, air or water operation. In such ambient conditions, SPMs have been stabilized using non-local sensors several centimeters away from the tip-sample location. Drift can be reduced by active stabilization using sensors closer to the tip, with the best results of ~ 0.5 nm in 3D.⁹ Many techniques could benefit from a *local*, high-bandwidth sensor of sample drift with excellent resolution. Such a sensor would allow a piezo-electric (PZT) stage to generate displacements that compensate for the locally measured drift.

Recently, we introduced a method that allows a single laser to measure the position of a reference mark on a sample in 3D with atomic-scale sensitivity.^{10, 11} By using the back-scattered optical signal from this reference mark – often called a fiducial mark – in a feedback loop, we actively minimized sample drift relative to the laser focus at room temperature in air (Fig. 1a). We introduce a second detection laser (Fig. 1b) that by design shares a largely collinear beam path with the initial laser. In this work, we used the second laser as an “out-of-loop” monitor to verify sample stabilization in the differential coordinate system between the laser foci. In future experiments, (Fig. 1c,d), we anticipate stabilizing the sample with respect to another object (i.e., optically trapped bead or AFM tip) detected by the second laser. Differential stability between the two lasers limits positional stability in these applications.

*tperkins@jila.colorado.edu; phone: 1 303 492-5291; fax: 1 303 492-5235

To fully exploit the high bandwidth provided by laser-based detection, the feedback rate should be limited by mechanical responses (e.g., PZT stage). In our prior work,¹⁰ the feedback rate was limited to 100 Hz by a software-based control algorithm. Additionally, this software-based feedback did not provide deterministic timing; disk writes, operating system interrupts, and graphical updates to the user interface led to timing glitches that degraded performance. In this work, we developed real-time, deterministic control using a field-programmable gate array (FPGA) for higher feedback rates that significantly improved lateral stability and enabled more sophisticated signal processing, yielding highly accurate orthogonal scanning.

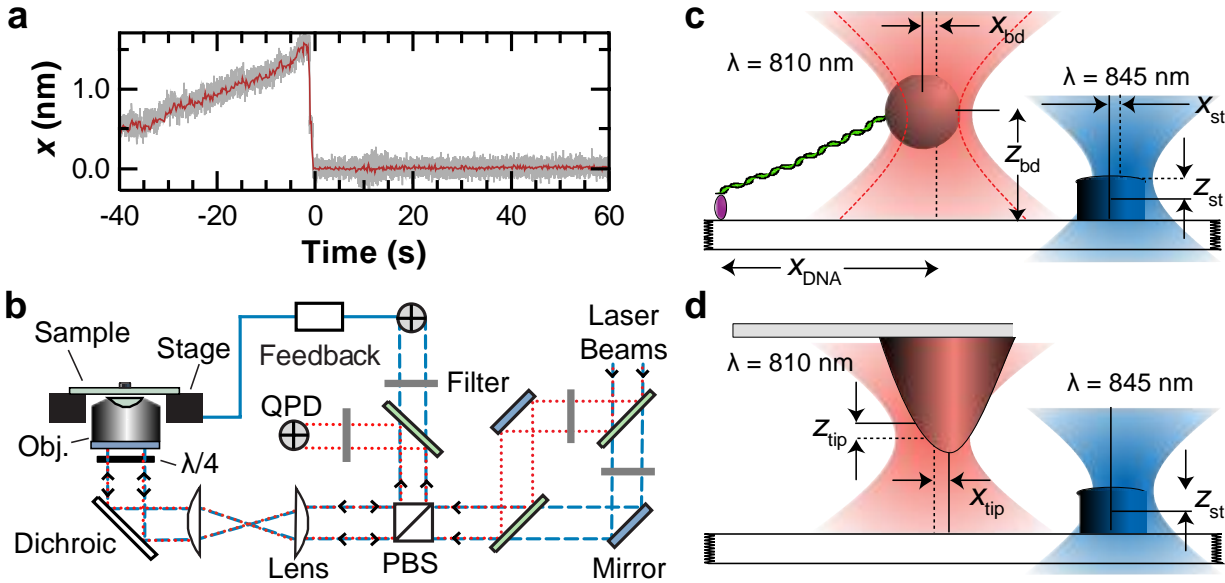


Fig. 1. (a) Stage position versus time was low-pass filtered to 500 Hz (*gray*) and 25 Hz (*red*). Initially, the stage position was not actively controlled. At $t = 0$, stabilization was turned on. (b) Schematic optical layout showing the feedback to the sample via a PZT stage. Reported sample traces were measured by one laser [810 nm (*red dotted lines*)]. Positions determined with a second laser [845 nm (*blue dashed lines*)] were used for feedback. Two potential applications of an ultrastable measurement platform are (c) optical tweezers (*trap represented by red dashed line*) and (d) atomic force microscopy. In both cases, one focused detector laser (*blue*) measures the sample position in 3D by scattering off a fiducial mark engineered into the sample. The second detector beam (*red*) scatters off of a probe, either an AFM tip or bead. The excellent differential stability between the lasers (~ 10 pm) establishes a local differential reference frame by which the relative probe/sample position remains constant.

2. INSTRUMENTATION

Use of backscattered detection from a nanofabricated fiducial mark to provide atomic-scale detection in 3D is described in detail elsewhere.¹⁰ Briefly, the backscattered signal was efficiently separated from the inward-propagating light by an optical isolator formed by a polarizing beam splitter (PBS) and a quarter waveplate ($\lambda/4$). Next, a dichroic mirror separated the signals onto two different quadrant photodiodes (QPD). Movement of the fiducial mark in x and y relative to the detector beam caused a corresponding change in the distribution of light on the QPD. Thus, the difference between the left and right halves measured the x signal, and the difference between the top and bottom halves yielded the y signal. However, there is some crosstalk, erroneous signal on one axis when moving another. Differential amplification and normalization electronics boosted the signal.¹¹ Although this work focused on lateral control, the vertical signal was obtained by using the total power measured on all quadrants of the QPD; vertical measurements can also achieve atomic-scale sensitivity¹⁰.

In this work, we used the position information from the back-scattered detection in an FPGA-based feedback loop. We controlled the sample position with a 3D, direct-drive, closed-loop PZT translation stage (Physik Instrumente, P-733.3DD, E-710). Feedback was performed using data acquisition and control software (National Instruments LABView 8.5). The FPGA chip (Xilinx Virtex-II) was contained in a PCI card (National Instruments PCI-7833R) along with memory, analog-to-digital and digital-to-analog converters, and input/output resources.

An FPGA chip mimics a dedicated patterned microchip by arranging blocks of logic to perform the requested task in hardware. Because it has a 40-MHz clock separate from the PC clock, the FPGA executes programs both quickly and with well-defined (i.e. deterministic) timing. As shown in Figure 2, all the functions required for the feedback loop were downloaded to the chip. The entire feedback loop was independent of the slower PC programs. This configuration allowed for higher feedback rates and deterministic timing. The limited logic resources of the FPGA chip constrain the complexity of the functions in the feedback loop. Additionally, fixed point numbers (64 bit) were used for on-chip calculations, as traditional floating point operations are not currently supported by the NI FPGA development software. Operations that are not time-sensitive (e.g., user interface, writing data to disk), executed on a desktop computer (Dell Dimension, 2.66 GHz Intel Core2Duo, LABView 8.5 under Windows XP).

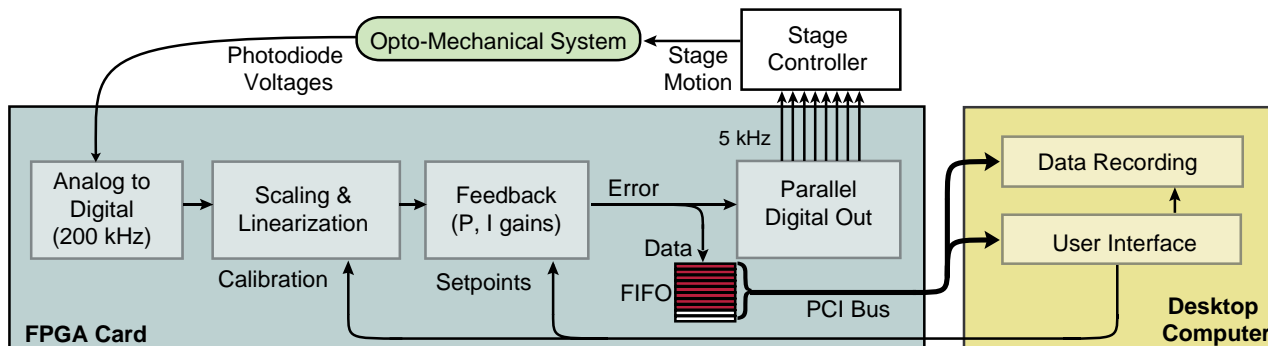


Fig. 2. Block diagram for FPGA feedback control. The FPGA digitizes incoming signals from the opto-mechanical system. Then, linear algebra routines scale and orthogonalize the optical detection to allow accurate feedback control on the separate x , y and z axes of the stage. Parallel digital output allows for high bandwidth communication with the stage controller. The FPGA passes the raw and scaled data to the host computer for display and recording. The host computer provides calibrations and overall interactive control via changes in the setpoints, and records the full bandwidth data for subsequent analysis.

The computational power of the FPGA allowed not only fast feedback but more complex mathematical operations. We took advantage of this computational power to minimize crosstalk using a routine adapted from optical trapping applications¹². Previously, each position (x , y , z) was parameterized in its corresponding voltage V_x using a polynomial of the form

$$x(V_x) = \sum_i a_i V_x^i \quad (1)$$

that does not take off-axis or cross terms into account. The present work utilized a 3D calibration, in which the reference mark was raster scanned in 3D through the detector beam. After this calibration, the backscattered signals (V_x, V_y, V_z) corresponding to stage movements could be scaled using a parameterization of the form

$$x(V_x, V_y, V_z) = \sum_{i,j,k=0}^{i+j+k=4} a_{ijk} V_x^i V_y^j V_z^k \quad (2)$$

for each axis x , y and z . Coefficients (a_{ijk}) were determined by a nonlinear least-square fitting routine to the aforementioned 3D calibration. Scaling the data at high speed according to this complex parameterization — 35 coefficients per axis for a fourth-order fit—was made possible by the high clock rate of the FPGA chip. Due to limited logic resources on the FPGA chip, we used a fourth order fit rather than the fifth order fits previously described.¹² The feedback signal was calculated with set points controlled from the host computer, which allows for scanning and, more broadly, interactive user-driven control. We used a standard proportional (P) and integral (I) control loop with $1 \leq P \leq 2$ and $0.01 \leq I \leq 0.02$. Control signals were sent directly to the stage controller via a 16-channel, fast (5 kHz) parallel output interface.

As the feedback loop executed, the raw and scaled data were written to first-in, first-out (FIFO) memory structures. Subsequently, the non-deterministic software (LABView) running on the desktop computer read from this FIFO enabling collection of lossless, high bandwidth data.

3. RESULTS

Future ultrastable scanning applications demand active atomic-scale control of the sample position, and we demonstrated the ability of our instrument to perform some foundational tasks. After first establishing the high lateral sample stability provided by FPGA control (10 pm), we next demonstrated rapid stabilized scanning (2 ms step duration). Finally, we show excellent orthogonal scanning over a large area using a computationally intensive, crosstalk-compensation algorithm. All of our results were determined by “out-of-loop” detection of the fiducial mark using the second detection laser. Thus, they are an accurate representation of the true performance within the differential measurement reference frame established by the pair of detector lasers.

3.1 Long-term lateral stability of 10 pm

Implementation of FPGA control significantly improved lateral stability performance (Fig. 3a, *color*). We compare these new results to prior results using slower (100 Hz) software-based feedback (Fig. 3a, *grey*). To quantify stability, we monitored the position of the fiducial mark for 100 s. We boxcar averaged the data within a 50 ms window, which preserves a 10 Hz frequency component. Next, we decimated the data to 20 points per second. This analysis yielded a standard deviation of 10 pm in both x and y . These results are more than a threefold improvement over prior results of 33 and 42 pm in x and y , respectively. A complementary analysis based on fitting histograms of the position records yielded identical results (Fig. 3b). Thus, our lateral stage control is sufficient for studying single atoms under ambient conditions and an order of magnitude smaller than the length of the OH bond in a water molecule (100 pm).¹³

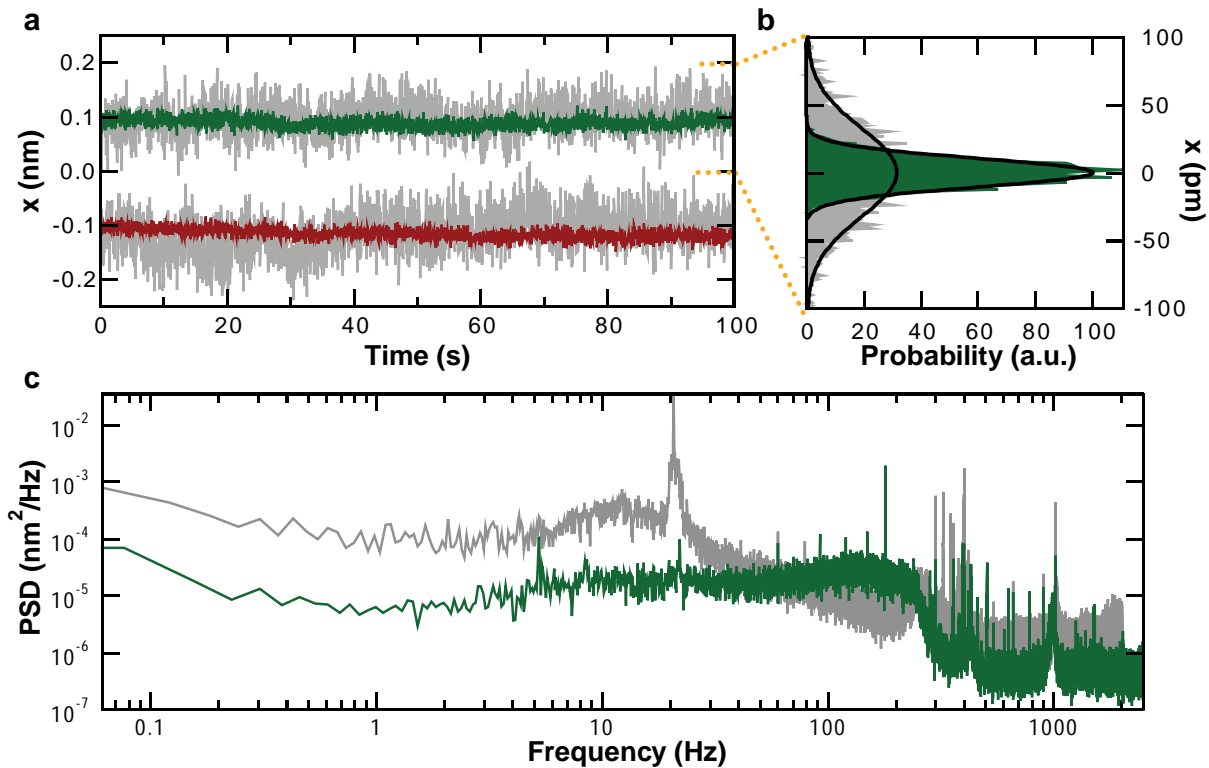


Fig. 3. Demonstration of improved performance provided by FPGA-based feedback control. (a) Lateral stabilization records (x , *dark green*; y , *dark red*) achieved with 500-Hz FPGA control in comparison to control achieved with 100 Hz software-based feedback (*light grey*). Both data sets are filtered to 10 Hz and offset for clarity. (b) Histograms of the x signal corresponding to the FPGA-based feedback and the software-based feedback are well fit by histograms with standard deviations of 10 and 33 pm, respectively. (c) Power spectral density analysis shows improvement in stability over a range of frequencies from 0.1 to 50 Hz (same color coding as in a).

FPGA-based control provided enhanced stability over a broad frequency range ($\Delta f = 0.1\text{--}50$ Hz). To demonstrate this improvement, we plot the power spectral density (PSD) of the stabilization records (Fig. 3c). At low frequencies (<20 Hz), we achieved PSDs that were an order of magnitude better than prior results, in agreement with the approximately threefold improvement in real space data, based on simple dimensional considerations (PSD is in units of nm^2/Hz , and $3^2 \approx 10$). An excellent alternative metric for calculating stabilities is to integrate the PSD within a specified bandwidth. We computed the integrated noise from 0.1 to 50 Hz, a broadly useful bandwidth for SPM and optical trapping experiments. The standard deviations were 30 and 28 pm for x and y , respectively. Calculating the equivalent metric on real-space data yields similar results as required by Parseval's Theorem. The results presented in Figure 3 used a proportionality gain of 2, which appears to have caused some excess noise at ~ 200 Hz. We have yet to fine tune the feedback loop parameters, and currently use only proportional and integral gain. Feedback loop parameter optimization should enhance performance.

3.2 Rapid stepping

Performance of advanced optical trapping and AFM experiments are improved by rapid, deterministic motion of the sample. For optical traps, such stage motion can maintain constant force on molecular motors.¹⁴ Higher bandwidth stage motion provides more accurate control of force. For AFMs, stepping is the basis of scanning for image acquisition and optical detection of sample motion provides for stabilized scanning.¹⁰

FPGA-based control enabled both rapid communication with the PZT stage controller and rapid stabilized stepping. As shown in Figure 2, communication between the FPGA and the stage controller was done using a parallel digital output. This communication protocol led to a 1 ms delay between the requested motion and its onset (*data not shown*). These requested changes in the stage position led to a staircase of 1 nm steps that were well resolved even at data filtered to 2 kHz. The nominal rise time (10–90%) per step was ~ 2 ms (Fig. 4, *inset*), which approaches the fastest step our stage (resonance frequency ~ 1000 Hz) could be expected to achieve. Thus, the overall delay between requesting and completing a step was 3 ms. We expect that optimization of the control code of the FPGA, faster stage controllers, and better feedback parameters can improve this delay by a factor of two. Further improvements will require stiffer stages with higher resonant frequencies.

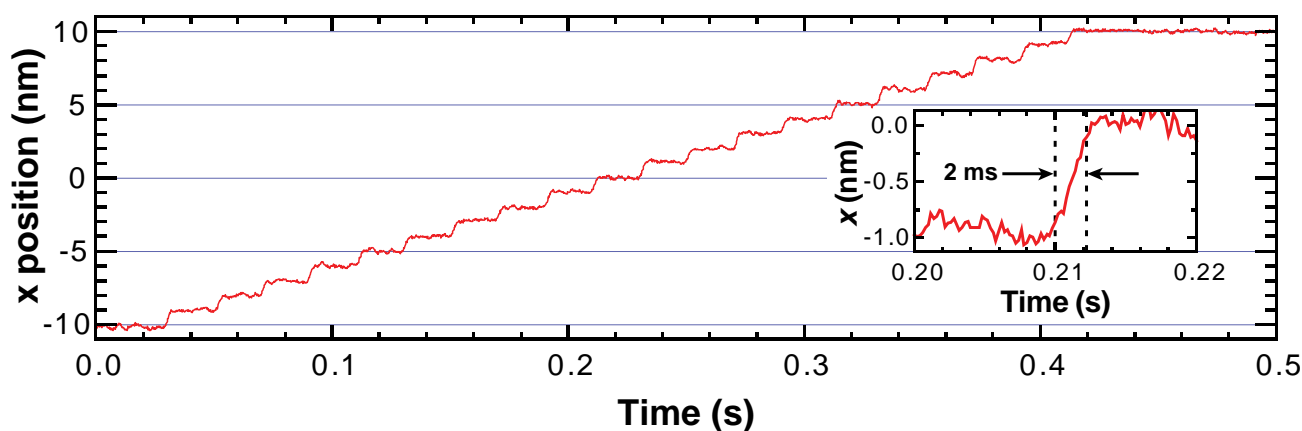


Fig. 4. Fast stepping enabled by parallel FPGA feedback control. (a) A record of sample position from a series of 1-nm steps filtered to 2 kHz. Sample position, independent of the servo-loop, was measured with the 845-nm laser. (Inset) Rise time for requested motion was ~ 2 ms with the total step completed ~ 3 ms after the request.

3.3 Highly orthogonal scanning

An ideal ultrastable measurement platform should provide both excellent stability in 3D about a particular location and accurate orthogonal scanning in all axes. Yet, optical crosstalk can lead to inaccurate positional control; motion in x leads to voltage changes in all three detection axes. Additionally, the QPD detection axes may not be perfectly aligned to the lateral axes of the PZT stage. More significantly, crosstalk increases as the reference mark is moved further out of the laser focus. Such crosstalk is well known from optical trapping experiments.^{12, 15} To address these issues, we adapted a previously published control algorithm¹² for use on an FPGA. Because of the computation speed provided by FPGA control, we were able to implement this cross-talk compensation algorithm without degradation of feedback bandwidth.

Crosstalk compensation significantly improved control of the stage position, particularly near the edges of the calibrated region, where discrepancies were more pronounced. To demonstrate the degree of improvement, we compared this difference in scanning control between linear fits ($x = a_1 V_x + a_0$) and fully cross-talk compensated detection (eq. 2) by moving the stage in a grid of points with 10 nm spacing over the entire $200 \times 200 \text{ nm}^2$ calibrated range, pausing at each point for $\sim 100 \text{ ms}$, and recording the x and y position as measured by the out of loop detector laser. We computed the average error (the difference between the requested and actual positions) in two regions. Near the center of the calibrated range (Fig. 2b, *blue region*), this test yielded an average residual error of 144 pm using a linear calibration versus 8 pm using full cross-talk compensation, an 18-fold improvement. Near the corner of the calibrated range (Fig. 2c, *red region*), a similar analysis yielded residual errors of 730 pm with the linear calibration versus 24 pm with the parameterization described in eq.2, a 30-fold improvement. Thus, the crosstalk compensation software allows for precise and accurate scanning over a much larger area while maintaining excellent sample stability.

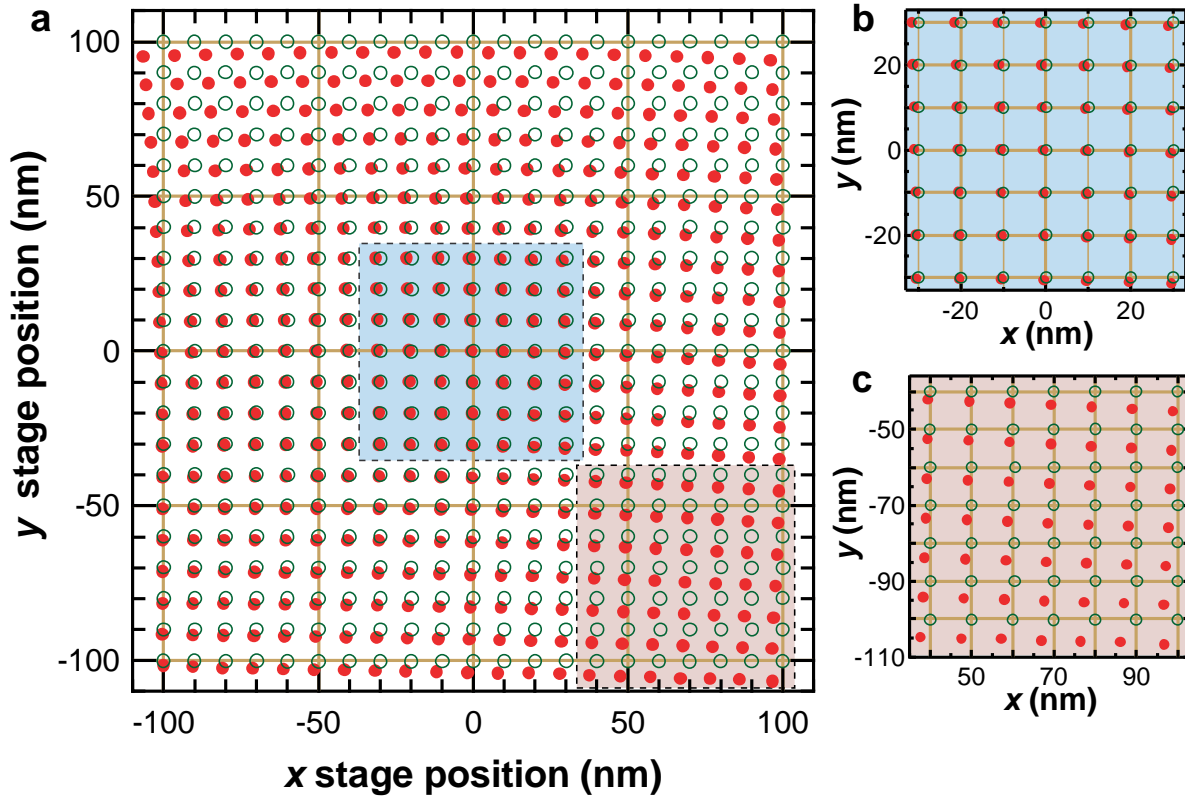


Fig. 5. (a) Two-dimensional scanning with (*open green circles*) and without (*closed red circles*) cross-talk compensation. Sample position, independent of the servo loop, was measured with the 845-nm laser. (b & c) Enlarged plots of the center and corner regions, respectively. (b) Scanning within a restricted area near the origin leads to less crosstalk. (c) Highly accurate scanning far from the origin was achieved with crosstalk compensation (*green*) while uncompensated points are subject to large systematic errors (*red*).

4. CONCLUSIONS

In this paper, we demonstrated a robust, ultrastable measurement platform based on local optical measurements in conjunction with real-time FPGA-based control of sample position. This feedback scheme provided atomic-scale active stabilization even in the presence of the large external perturbations due to ambient operating conditions. The approach relied on precise optical measurement of sample position local to the measurement point. A FPGA-PCI card then rapidly processed these optically generated voltages into position and generated orthogonalized error signals. Communication occurred in parallel to the sample stage controller, allowing for rapid movement in all three axes. Furthermore, this control occurred in real time, buffered from the indeterminacies of the operating system and other interrupts. With this FPGA system, we achieved a threefold improvement over our prior software-based stabilization results. This degree of lateral localization stability (10 pm) represents an order-of-magnitude enhancement over the manufacturer's nominal

(100 pm) resolution of the stage. We have also demonstrated the added benefit of a full 3D optical calibration for highly linearized and orthogonal control over a $200 \times 200 \times 100 \text{ nm}^3$ calibrated range. Looking forward, we expect that the intrinsically parallel and deterministic control provided by FPGA architecture will become increasingly valuable for future precision nanoscience applications, such as optically stabilized AFM, that demand real time control of many (>3) independent axes. Moreover, as newer generations of FPGA-PCI cards become available, they will likely provide higher feedback bandwidths coupled with more reconfigurable logic blocks that will allow for high-precision displacements over a larger dynamic range.

Acknowledgments

The authors thank Scott Jordan for technical discussion and for FPGA-based parallel communication software, Joshua Shaevitz and Charles Asbury for crosstalk compensation software. This work was supported by separate Burroughs Wellcome Fund Career Awards to GMK and TTP, a National Research Council Research Associateship (GMK), an Optical Science and Engineering Program NSF-IGERT Grant (ARC), a National Physical Science Consortium Fellowship (ARC), a Butcher Grant (TTP), the National Science Foundation (TTP, Phy-0404286) and NIST. Mention of commercial products is for information only; it does not imply NIST's recommendation or endorsement, nor does it imply that the products mentioned are necessarily the best available for the purpose. TTP is a staff member of NIST's Quantum Physics Division.

References

- [1] Denk, W. and Webb, W. W., "Optical measurement of picometer displacements of transparent microscopic objects," *Appl. Opt.* **29**(16), 2382-2391 (1990).
- [2] Binnig, G., Quate, C. F. and Gerber, C., "Atomic Force Microscope," *Phys. Rev. Lett.* **56**(9), 930-933 (1986).
- [3] Binnig, G., Rohrer, H., Gerber, C. and Weibel, E., "7X7 Reconstruction on Si(111) Resolved in Real Space," *Phys. Rev. Lett.* **50**(2), 120-123 (1983).
- [4] Abbondanzieri, E. A., Greenleaf, W. J., Shaevitz, J. W., Landick, R. and Block, S. M., "Direct observation of base-pair stepping by RNA polymerase," *Nature* **438**(7067), 460-465 (2005).
- [5] Thomson, N. H., Fritz, M., Radmacher, M., Cleveland, J. P., Schmidt, C. F. and Hansma, P. K., "Protein tracking and detection of protein motion using atomic force microscopy," *Biophys. J.* **70**(5), 2421-2431 (1996).
- [6] Nugent-Glandorf, L. and Perkins, T. T., "Measuring 0.1-nm motion in 1 ms in an optical microscope with differential back-focal-plane detection," *Opt. Lett.* **29**(22), 2611-2613 (2004).
- [7] King, G. M. and Golovchenko, J. A., "Probing nanotube-nanopore interactions," *Phys. Rev. Lett.* **95**(21), 216103 (2005).
- [8] Stipe, B. C., Rezaei, M. A. and Ho, W., "Single-molecule vibrational spectroscopy and microscopy," *Science* **280**(5370), 1732-1735 (1998).
- [9] Moon, E. E. and Smith, H. I., "Nanometer-precision pattern registration for scanning-probe lithographies using interferometric-spatial-phase imaging," *J. of Vac. Sci. Technol. B* **24**, 3083-3087 (2006).
- [10] Carter, A. R., King, G. M. and Perkins, T. T., "Back-scattered detection provides atomic-scale localization precision, stability, and registration in 3D," *Opt. Express* **15**(20), 13434-13445 (2007).
- [11] Carter, A. R., King, G. M., Ulrich, T. A., Halsey, W., Alchenberger, D. and Perkins, T. T., "Stabilization of an optical microscope to 0.1 nm in three dimensions," *Appl. Opt.* **46**(3), 421-427 (2007).
- [12] Lang, M. J., Asbury, C. L., Shaevitz, J. W. and Block, S. M., "An automated two-dimensional optical force clamp for single molecule studies," *Biophys. J.* **83**(1), 491-501 (2002).
- [13] Kusalik, P. G. and Svishchev, I. M., "The Spatial Structure in Liquid Water," *Science* **265**(5176), 1219-1221 (1994).
- [14] Perkins, T. T., Dalal, R. V., Mitsis, P. G. and Block, S. M., "Sequence-dependent pausing of single lambda exonuclease molecules," *Science* **301**(5641), 1914-1918 (2003).
- [15] Neuman, K. C. and Block, S. M., "Optical trapping," *Rev. Sci. Instrum.* **75**(9), 2787-2809 (2004).